



**HAL**  
open science

## Solubility and dissolution performances of spray-dried solid dispersion of Efavirenz in Soluplus

Zênia Maria Maciel Lavra, Davi Pereira De Santana, Maria-Inês Ré

### ► To cite this version:

Zênia Maria Maciel Lavra, Davi Pereira De Santana, Maria-Inês Ré. Solubility and dissolution performances of spray-dried solid dispersion of Efavirenz in Soluplus. *Drug Development and Industrial Pharmacy*, 2017, 43 (1), p.42-54. 10.1080/03639045.2016.1205598 . hal-01619242

**HAL Id: hal-01619242**

**<https://hal.science/hal-01619242v1>**

Submitted on 16 Oct 2020

**HAL** is a multi-disciplinary open access archive for the deposit and dissemination of scientific research documents, whether they are published or not. The documents may come from teaching and research institutions in France or abroad, or from public or private research centers.

L'archive ouverte pluridisciplinaire **HAL**, est destinée au dépôt et à la diffusion de documents scientifiques de niveau recherche, publiés ou non, émanant des établissements d'enseignement et de recherche français ou étrangers, des laboratoires publics ou privés.

# Solubility and dissolution performances of spray-dried solid dispersion of Efavirenz in Soluplus<sup>®</sup>

Lavra, Zênia Maria Maciel<sup>1,2</sup>; Santana, Davi Pereira<sup>2</sup>; Ré, Maria Inês<sup>1\*</sup>

<sup>1</sup>Mines Albi, CNRS, Centre RAPSODEE, Campus Jarlard, Université de Toulouse, 81013 Albi CT Cedex 09, France

<sup>2</sup>Department of Pharmaceutics Sciences, Faculty of Pharmacy, Federal University of Pernambuco, Pernambuco, PE, Brazil.

**\*Corresponding author:**

e-mail : maria-ines.re@mines-albi.fr

Tel: (33) 5 6349 3299; Fax: (33) 5 6349 3025

## **Abstract**

Efavirenz (EFV), a first-line anti-HIV drug largely used as part of antiretroviral therapies, is practically insoluble in water and belongs to BCS class II (low solubility/high permeability). The aim of this study was to improve the solubility and dissolution performances of EFV by formulating an amorphous solid dispersion of the drug in polyvinyl caprolactam-polyvinyl acetate-polyethylene glycol graft copolymer (Soluplus<sup>®</sup>) using spray-drying technique. To this purpose, spray-dried dispersions of EFV in Soluplus<sup>®</sup> at different mass ratios (1:1.25, 1:7, 1:10) were prepared and characterized using particle size measurements, SEM, XRD, DSC, FTIR and Raman microscopy mapping. Solubility and dissolution were determined in different media. Stability was studied at accelerated conditions (40°C/75%RH) and ambient conditions for 12 months. DSC and XRD analyses confirmed the EFV amorphous state. FTIR spectroscopy analyses revealed possible drug polymer molecular interaction. Solubility and dissolution rate of EFV was enhanced remarkably in the developed spray-dried solid dispersions, as a function of the polymer concentration. Spray-drying was concluded to be a proper technique to formulate a physically stable dispersion of amorphous EFV in Soluplus<sup>®</sup>, when protected from moisture.

**Keywords:** Efavirenz amorphous; solid dispersion; spray drying; dissolution; drug solubility, stability

## Introduction

Efavirenz (EFV) is a first-line anti-HIV drug largely used as a non-nucleoside reverse transcriptase inhibitor as part of antiretroviral therapies. The recommended dosage in adults is 600 mg once daily. Despite being widely used clinically, this drug has very low aqueous solubility (below 10 $\mu$ g/mL)<sup>1</sup>, low oral bioavailability (40-45%) and high inter-individual (56%) and intra-individual (22%) variability in its absorption<sup>2</sup>.

EFV is commercially available in micronized crystalline form. Studies available in the literature have been dedicated to the improvement of the drug solubility and to the sustained release of EFV<sup>3,4,5</sup>. The published works about the solutions to increase the solubility of EFV are focusing on micronization<sup>6</sup>, co-micronization of EFV with dispersant agents such as sodium lauryl sulfate (SLS) or polyvinylpyrrolidone (PVP)<sup>7</sup>, nano-crystals<sup>8</sup>, complexation with cyclodextrins<sup>9,10</sup>, encapsulation of EFV in polymeric micelles<sup>11</sup>, Self-Micro-emulsifying Drug Delivery System (SMEDDS)<sup>12</sup> and co-crystals<sup>13</sup>.

The approach of formulating amorphous EFV in the form of solid dispersions with a polymeric carrier as a crystallization inhibitor has also been an active area of research. Polyethylene glycol<sup>14,15</sup>, PVP K-30<sup>16</sup>, Eudragit EPO or Plasdone S-630<sup>17</sup> as well as new modified starches named starch citrate and starch phosphate<sup>18</sup> have been used as hydrophilic carriers. Despite the progress already made, the development of a considerable number of stable and efficient formulations is yet to be achieved. The major challenge is to obtain molecule-level dispersions restraining favorable intermolecular interactions between EFV and the polymeric matrix.

For the current study the solubilizing potential of the polyvinyl caprolactam-polyvinyl acetate-polyethylene glycol graft copolymer (Soluplus<sup>®</sup>) was explored. This polymer offers exceptional capabilities for solubilization of BCS class II drugs due to its bi-

functional nature. It is considered as a member of the fourth generation of solid dispersion because of its bifunctional character, acting as an active solubilizer through micelle formation in water<sup>19</sup>. Soluplus<sup>®</sup> is ideal for hot-melt extrusion (HME) with excellent extrudability and easy processing<sup>20</sup> however, to the best of our knowledge, this is the first attempt to develop Efavirenz-Soluplus<sup>®</sup> amorphous solid dispersion by spray drying.

HME and spray drying are capable of being scaled-up into large manufacturing scale<sup>21,22,23</sup>.

Different physical solid structures are generated from these two different processes. It is important to correlate the physical structure of the drug-polymer dispersions to their pharmaceutical performance and stability profile, and to correlate formulation and processing parameters to the resulting physical structure. This study aimed then at assessing particle generation in spray drying and its effect on solubility, dissolution and stability performance by varying different drug: polymer ratios, namely 1:1.25; 1:7 and 1:10 (w/w). The spray-dried EFV-Soluplus<sup>®</sup> particles were evaluated with respect to particle size, morphology, solid-state properties, solubility and *in vitro* drug dissolution in various aqueous media and stability during storage under controlled conditions of temperature and humidity.

## **Materials and Methods**

### ***Materials***

Efavirenz (EFV) ((S)-6-chloro-4-(cyclopropylethynyl)-1,4-dihydro-4-(trifluoromethyl)-2H-3,1-benzoxazin-2-one, structural formula given in Fig. 1a) was kindly supplied by Cristalia Ltd (Itapira, Brazil). Soluplus<sup>®</sup> (polyvinyl caprolactam-polyvinyl acetate-

polyethylene glycol graft copolymer/PCL-PVAc-PEG, structural formula given in Fig. 1b, with the average molecular weight ranging from 90,000 to 140,000g/mol, was donated by BASF Corporation (Ludwigshafen, Germany).

Ethanol 99% (Carlo Erba, Italy) was applied as solvent in the preparation of solid dispersions. Acetonitrile chromatographic grade was purchased from Merck (Frankfurter, Germany), Ammonium acetate and sodium lauryl sulfate (SLS) were acquired from Vetec (Rio de Janeiro, Brazil). Buffer solutions and dissolution media were prepared using purified water (Millipore, Bedford, MA, USA).

## ***Methods***

### **Preparation of Spray-Dried Solid Dispersions (SDSD) of EFV in Soluplus<sup>®</sup>**

Spray drying was used as the process to prepare solid dispersions of EFV in Soluplus<sup>®</sup> at various compositions corresponding to drug: polymer mass proportions of 1:10; 1:7 and 1:1.25.

A Buchi B-290 minispray drier (Buchi Labortechnik AG, Flawil, Switzerland) equipped with Inert Loop B-295 and an integrated two-fluid 0.7 mm nozzle was used for spray drying. Compressed nitrogen dispersed the liquid into fine droplets, which were consequently dried in the drying chamber and deposited in the cyclone. Drying conditions are given as follows for all prepared samples: aspirator 100%; pump flow rate 300 ml/h and compressed nitrogen flow rate 600 l/h. The inlet temperature was set to 70±1°C and the outlet temperature at 62±3°C. The experiments were made in duplicate.

The feeding solution was prepared by dissolving EFV in a 10 (w/w) % solution of Soluplus<sup>®</sup> in ethanol. Ethanol was the first-choice solvent in this study based on four criteria (high solubility of API and polymer, the generation of a feed solution with

acceptable viscosity, low toxicity and high volatility for the ease of solvent evaporation during droplet drying)<sup>24</sup>.

The individual constituents (drug and polymer) were also spray-dried from ethanol solutions. They were used for comparison purposes. All obtained powders were collected in glass containers and stored at room temperature in vacuum desiccators till further studies.

In addition, physical mixtures were prepared in the drug: polymer mass proportion of 1:1.25 by mixing EFV and the polymer in a mortar for about 3 min.

## **Characterization methods**

### ***Solubility parameters ( $\delta$ ) and Gordon-Taylor calculations***

As a preliminary indicator of the drug-polymer miscibility, the Hansen solubility parameters ( $\delta$ )<sup>25</sup> were calculated from their chemical structures using the Hoftyzer and Van Krevelen group contribution method<sup>2</sup> according to Eq. 1:

$$\delta = (\delta_d^2 + \delta_p^2 + \delta_h^2)^{1/2} \quad (\text{Eq. 1})$$

where:

$$\delta_d = \frac{\sum_i Fdi}{V}; \quad \delta_p = \frac{\sqrt{\sum_i F^2 pi}}{V}; \quad \delta_h = \sqrt{\frac{\sum_i Ehi}{V}}$$

V is the molar volume and Fdi, Fpi and Ehi are the group contributions for different component (dispersion forces, polar interactions and hydrogen bonding, respectively) of structural groups that are reported in the literature<sup>26</sup>.

A binary mixture containing components with a considerable difference between individual glass transition temperature (Tg) values, if the drug and the polymer are miscible, will exhibit only one Tg which is intermediate between those of the pure

components and dependent on the relative proportion of each component. The position of T<sub>g</sub> for a miscible but not interactive system with merely equivalent cohesive and adhesive contributions between individual components can be estimated using various equations that follow a simple rule of mixing, among them the Gordon-Taylor (GT) equation. This equation is based on weight fractions, densities and T<sub>g</sub> of pure components, as described by Eq. 2<sup>27</sup>:

$$T_{g \text{ mix}} = \frac{(W_1 T_{g1} + K W_2 T_{g2})}{W_1 + K W_2} \quad (\text{Eq. 2})$$

where,

$$K = \frac{T_{g1} \rho_1}{T_{g2} \rho_2}$$

In this equation, T<sub>g1</sub> and T<sub>g2</sub> are the glass transition temperatures of drug and polymer, W<sub>1</sub> and W<sub>2</sub> are the weight fractions of the constituents of the mixture and the constant K is calculated by the true densities ρ<sub>1</sub> (drug) and ρ (polymer). The true densities of EFV (1.39 ± 0.01 g/cm<sup>3</sup>) and Soluplus<sup>®</sup> (1.18 ± 0.005 g/cm<sup>3</sup>) were determined in duplicate using a gas displacement pycnometer (Accupyc 1330-Micromeritics, Germany).

The GT equation was used to predict the theoretical T<sub>g</sub> of the spray-dried solid dispersions. These values were compared to the experimentally determined T<sub>g</sub> obtained during the first DSC heating cycle.

### ***Thermal analyses***

Thermal analyses were performed using a differential scanning calorimeter DSC Q200 with the base module and modulate-DSC (TA Instruments, USA). Samples of EFV and SDS binary systems were heated in non-hermetic aluminum pans at a rate of 5°C/min in 20 to 190 °C temperature range under nitrogen flow of 50 ml/min using an empty sealed pan as reference. DSC modulated technique (mDSC) was used because of its



capacity to increase the resolution and the sensibility for weak transitions. In mDSC experiments, the samples were heated at a sinusoidal program of 2°C/min from 20 to 150°C, with the modulation period of 40s and amplitude 0.2°C.

### ***X-ray powder diffraction***

X-ray powder diffractions were recorded on X'Pert Pro MPD X-ray diffractometer (Philips, USA) using CuK $\alpha$  radiation, applying 45 kV of voltage and a 40 mA current. The scanning rate employed was 0.018°/min over the diffraction angle ( $2\theta$ ) range from 5 to 40°.

### ***Fourier Transform Infrared Spectroscopy (FTIR)***

The FTIR were recorded using Nicolet 5700 spectrometer (Thermo Scientific, USA). Samples of unprocessed EFV crystals, Soluplus<sup>®</sup> and SDDS systems were ground and mixed thoroughly with potassium bromid (KBr) at 1-2% (w/w) of the samples in KBr and the discs were prepared by compressing the powders at a working pressure of 1 ton. The scanning range was 4000 to 400 cm<sup>-1</sup> with a spectral resolution of 4 cm<sup>-1</sup>.

### ***Particle size, morphology and yields of SDDS EFV-Soluplus<sup>®</sup>***

Particle size distributions were determined using a laser diffraction particle size analyzer (Mastersizer 2000, Malvern Instruments, UK). Average particle size was expressed as the volume mean diameter [D4.3]. Polydispersity was given by Span index calculated by  $(Dv_{90} - Dv_{10})/Dv_{50}$ , where  $Dv_{90}$ ,  $Dv_{50}$  and  $Dv_{10}$  are the particle diameters determined respectively at the 90th, 50th and 10th percentiles of undersized particles. The measurements were performed in quintuplicate. Morphological evaluation of

unprocessed EFV crystals and SDS samples was performed by Scanning Electron Microscopy (SEM) using Philips XL30 FEG (Philips, USA) with beam accelerating voltage of 20 kV. The samples were fixed on aluminum stubs, sputtered with gold using a Polaron SC7640 high vacuum sputtering device (Quorum Technology, England) and analyzed by SEM.

The yields of spray dried samples were calculated by determining the weight of recovered particles divided by the total original weight of EFV and Soluplus.

### ***Solubility studies***

The solubility of the unprocessed EFV crystals and the apparent solubility of the SDS samples was measured in purified water, in purified water containing 0.25 (w/v) % SLS and in biorelevant medium (FeSSIF). The latter was composed of sodium chloride (203 mM), sodium hydroxide (101 mM), lecithin (3.75 mM) and sodium taurocholate (15 mM) and was based on a partly physiological acetate buffer (0.144 M, pH 5.0) to simulate the feed state intestinal fluid.

For solubility studies, an excess amount of powder samples were added into 15 mL of each dissolution medium in test tubes. The tubes were kept under agitation at  $37 \pm 0.5^\circ\text{C}$  (water bath Dubnoff, Quimis, Brazil). After 48 h, the supernatants were collected and centrifuged at 4000 rpm for 5 min, filtered through 0.45  $\mu\text{m}$  membrane filters (Whatman International, England), and then assayed by UHPLC. Measurements were made in triplicate and values were expressed as mean  $\pm$  standard deviations (SD).

### ***In vitro drug dissolution***

#### ***Dissolution testing***

In vitro drug release experiments were carried out in an automated dissolution system (Varian VK7010 with autosampler VK 8000, Lexington MA 02421, USA) equipped with rotating paddles (Apparatus 2)<sup>28</sup>. The test was performed at 37±0.5°C and stirring rate of 50 rpm. Two dissolution media (900 mL) were tested: purified water containing 0.25 (w/v) % SLS and FeSSIF medium. The two dissolution media were tested because sodium lauryl sulfate is described as the solid wetting agent of choice for EFV dissolution testing<sup>29</sup>. However, biorelevant media as FeSSIF is also of interest to anticipate potential food effects<sup>30</sup>.

To ensure the same sink conditions (EFV concentration three times lower than the equilibrium concentration of the drug in each medium), samples equivalent to 100 mg of EFV were used in each test carried out in 0.25 (w/v) % SLS, whereas a quantity equivalent to 250 mg of EFV was used in the tests performed in FeSSIF medium. A suitable amount of sample (3mL) was collected at 2, 5, 8, 10, 15, 20, 30, 60 and 120 min, filtered using syringe filter with a 0.45 µm pore size PTFE membrane. The concentration of EFV in the dissolution medium was measured by UHPLC (Shimadzu Nexera, Japan). Measurements were made in triplicate and values were expressed as mean ± SD.

#### *Methods used to compare EFV release profiles from SDSD EFV-Soluplus<sup>®</sup>*

Drug release profiles were analyzed using model-dependent (curve-fitting) and independent approaches (Dissolution Efficiency-DE). The free open source software KinetDS<sup>®31</sup> was used to fit the release curves to the Korsmeyer-Peppas mathematical model :

$$Mt = K_{KP} \cdot t^n \quad (\text{Eq. 3})$$

where  $M_t$  is the amount of drug released in time  $t$ ;  $K_{KP}$  is the release constant incorporating structural and geometric characteristics of the drug-dosage form and  $n$  is the diffusional exponent indicating the drug-release mechanism.

Korsmeyer-Peppas model is a semi-empirical model, relating exponentially the drug release to the elapsed time. It is used to analyze the release of pharmaceutical polymeric dosage forms, when the release mechanism is not well known or when more than one type of release phenomenon could be involved<sup>32</sup>. The accuracy and prediction ability of the mathematical model were analyzed by calculation of coefficient of determination ( $R^2$ ), RMSE (root mean square error) and AIC (Akaike's information criterion) described by Eq. 4 and 5, respectively:

$$RMSE = \sqrt{\frac{\sum_{i=1}^n (y_{iobs} - y_{ipred})^2}{n}} \quad (\text{Eq. 4})$$

$$AIC = 2k + n \cdot [\ln(\sum_{i=1}^n (y_{iobs} - y_{ipred})^2)] \quad (\text{Eq. 5})$$

The dissolution efficiency (DE) was calculated by KinetDS<sup>®</sup> according to Eq. 6:

$$DE = \left( \frac{\int_0^t M_t dt}{M_{tmax.t}} \right) \times 100 \quad (\text{Eq. 6})$$

where  $M_{tmax}$  is the maximum amount of drug released (=100%).

The differences for DE were statistically examined by one-way ANOVA followed by Tukey's test in order to find the source of difference. In this method,  $\langle DE \rangle$  ( $n=2$ ) was the dependent variable, and  $\langle \text{Formulation} \rangle$  was the factor. The calculations were performed using *Matlab*. Throughout the study,  $p \leq 0.05$  was used as the criterion to assess statistical significance.

### ***Drug quantification***

All samples (solubility measurements, drug content and dissolution profiles) were analyzed by UHPLC (Shimadzu Nexera, Japan) according to the method approved by the MD-AA Expert Committee (USP) as an Authorized USP Pending Standard. The analytical method was based on an isocratic elution system with a buffer ammonium acetate pH 7.5 (adjusted with diluted ammonia solution) and acetonitrile (30:70 v:v) mobile phase, chromatographic column Phenomenex® Luna C18, 25cm x 46 mm, 5µm kept at 40°C. The flow rate of 1.5ml/min resulted in a retention time of 3.7 min. Twenty microliters samples were injected and detection wavelength was set at 252 nm. For drug content analysis, an amount of sample (10mg) was weighed accurately and dissolved in 50 ml acetonitrile. The solution was sonicated for 15 min and diluted with suitable quantity of acetonitrile to 20µg/ml. For solubility and dissolution measurements, the samples were collected and directly injected into UHPLC after filtration. All studies were carried out in triplicates and values were expressed as mean ± SD.

### ***Stability studies***

#### *Dynamic vapor sorption (DVS)*

A DVS was used to monitor the water sorption capacities of the powders. Water sorption isotherms were determined gravimetrically using an automated water sorption analyzer (DVS-2, Surface measurement systems Ltd., London, UK). The DVS-2 measures the uptake and loss of vapor gravimetrically using a recording microbalance. The relative humidity around the sample was controlled by mixing saturated and dry carrier gas streams using mass flow controllers. The temperature was kept constant at 25°C. Prior to being exposed to any water vapor, the sample was dried at 0% RH to remove any water present. Next, the sample was exposed to the desired relative

humidity and the moisture uptake was measured. More specifically, approximately 100 mg of sample was weighed into the sample pan of the DVS and subjected to one 0–90% relative humidity (RH) sorption-desorption cycle, over 10% RH increments. Equilibrium sorption at each humidity step was determined by a change in mass to time ratio of 0.007 dm/dt.

In a complementary study using DVS-2, the solid dispersion most concentrated in drug (SDSD3) was exposed to 40°C/75% RH until its moisture content reaches equilibrium. The sample was then immediately analyzed, in a coordinated manner, by DSC and Raman microscopy mapping (Alpha 300R Raman-AFM spectrophotometer, WITEC GmbH, Germany) to monitor changes in the physical state. The samples were dispersed on a glass slide and the analyses were conducted at room temperature using a confocal laser wavelength of 532 nm (Nd:YAG laser) and ultrahigh-throughput (UHTS 300) spectroscopy system with a CCD (charge-coupled device) as detector. Spectra images were the average of 10 scans taken within of a selected area.

#### *Long-term stability*

SDSD samples were stored in desiccator at approximately 23% RH and 22°C. The solid dispersions were characterized by DSC and XRD analyses after storage for 12 months.

## **Results and Discussion**

#### *Miscibility analysis based on $\delta$ and $T_g$ values*

Based on the molecular structure, the solubility parameters ( $\delta$ ) for EFV and Soluplus<sup>®</sup> were calculated to be 24.5 MPa<sup>1/2</sup> and 19.8 MPa<sup>1/2</sup>, respectively (data not shown). It is

generally believed that favorable interactions and a uniform phase will result when the difference in  $\delta$  values between two components ( $\Delta\delta$ ) is less than  $7 \text{ MPa}^{1/2}$ , while unfavorable interactions and phase separation will result when  $\Delta\delta > 10 \text{ MPa}^{1/2}$ <sup>33</sup>. In the present case,  $\Delta\delta$  between Soluplus<sup>®</sup> and EFV was of  $4.7 \text{ MPa}^{1/2}$  and EFV is likely to be miscible with Soluplus<sup>®</sup> in the SDS systems.

The thermal properties of the individual components and the SDS systems containing drug-to-polymer mass proportions of 1:10 (SDS1), 1:7 (SDS2) and 1:1.25 (SDS3) are given in Table 1. All DSC analyses are grouped in Fig. 2 to ease data analysis. Fig. 1 also shows the DSC thermogram of the physical mixture between EFV and Soluplus<sup>®</sup> in a mass proportion of 1:1.25.

The thermal profile of unprocessed EFV crystals shows a distinct melting endotherm ( $T_m$ ) at  $139.2^\circ\text{C}$  with a  $\Delta H_m$  of  $51.9 \text{ J/g}$ . This value of  $T_m$  is close to that reported in the literature for the most thermodynamically stable crystalline form of EFV ( $138\text{-}140^\circ\text{C}$ )<sup>34</sup>. As shown in Table 1, the amorphous drug obtained by spray-drier exhibits a low  $T_g$  of  $36.1^\circ\text{C}$ , whereas amorphous Soluplus<sup>®</sup> has a  $T_g$  of  $78.8^\circ\text{C}$ , consistent with previously reported data<sup>35</sup>.

Active pharmaceutical ingredients (APIs) that demonstrate good glass-forming properties have  $T_g/T_m$  (in Kelvin) ratio greater than 0.67 (i.e., the rule of 2/3rds) according to the Boyer-Beaman rule<sup>35,36</sup> in order to form solid dispersions. Therefore, with a  $T_g/T_m$  (in Kelvin) of 0.75, EFV is expected to be able to form solid dispersions.

In Fig. 1, the physical mixture exhibits the endotherm for melting of EFV indicating the presence of EFV crystals not dissolved in the polymer under the thermal analysis conditions. Contrarily, thermograms for the spray dried mixtures of EFV-Soluplus<sup>®</sup> at 1:1.25, 1:7, 1:10 mass ratios (Fig. 1) reveal the absence of the EFV melting endotherm. This analysis proves that Soluplus<sup>®</sup>, even at a 1:1.25 drug-polymer mass ratio,

successfully dispersed EFV with no trace of crystallinity when the spray drying method was used.

In addition, distinctive and single  $T_g$  without other noticeable events were observed in the reversing heat flow signals for all freshly prepared SDSD systems (Fig. 1, Table 1). From the recorded data, it can be seen that the  $T_g$  values increased from 58.1°C to 62.3°C, as the polymer mass proportion increased from 1:1.25 to 1:10 in the formulation. Table 2 also compares experimental  $T_g$  and theoretical  $T_g$  calculated by GT equation (Eq. 2) as a function of the mixture composition. GT equation has been used to predict the glass transition temperature of blends. The predicted  $T_g$  for any mixture matches the experimental data if two conditions are met: mixing occurring at the molecular level (ideal mixing) and no changes in the volume during mixing. However, for all SDSD samples, the experimental  $T_g$  values are lower than the theoretical value determined by the GT equation. Such deviation may be due to non-ideal mixing in reason of an unexpected change in volume. Other possible explanations for these negative  $T_g$  deviations include: 1) difference in the molecular interaction (if attractive forces between the drug and the polymer are weaker than self-associating interactive drug-drug or polymer polymer forces<sup>37</sup>; 2) residual solvent effects.

#### *X-ray powder diffraction (XRD)*

The physical state of EFV in the solid dispersions was further investigated by XRD analyses. The powder XRD patterns for unprocessed EFV crystals, Soluplus<sup>®</sup> and SDSD samples are shown in Fig 2. XRD pattern for pure EFV presented several diffraction peaks indicating the crystalline nature of the drug. The principal intense crystalline peaks occurring at diffraction angles ( $2\theta$ ) as 6.20°, 20.20°, 21.35° and 25.00° can be identified, similar to those reported in the literature for this drug<sup>34</sup>. The XRD



pattern of Soluplus<sup>®</sup> was characterized by a complete absence of any diffraction peak, which confirms its amorphous nature. The diffraction patterns of SDSD samples prepared by spray drying showed absence of peaks, which indicated that EFV lost its regular ordered lattice structure, becoming amorphous during the spray drying process. XRD observations are in good agreement with DSC confirming the amorphization of EFV in SDSD1, SDSD2 and SDSD3 samples.

#### *Fourier Transform Infrared Spectroscopy (FT-IR)*

The EFV molecule presents the N-H group considered H<sup>+</sup> donor (N-H) and acceptor groups (C=O and -O-). Soluplus<sup>®</sup> has functional groups C=O as acceptor of hydrogen<sup>38</sup>, which could favor interactions with EFV by hydrogen bonds. In order to evaluate any possible chemical interactions between EFV and Soluplus<sup>®</sup>, FTIR spectra of the pure components and SDSD systems are presented in Fig. 3 IR spectrum of EFV presented characteristic peaks at 3320 cm<sup>-1</sup> (N-H stretching vibrations), 2250cm<sup>-1</sup> (C≡C stretching vibrations), 1750 cm<sup>-1</sup> (C=O stretching vibrations), 1600 cm<sup>-1</sup> (N-H bending vibrations) and around 1250 cm<sup>-1</sup>(stretching vibrations C-F)<sup>17,39</sup>. Soluplus<sup>®</sup> exhibited characteristic absorption peaks at 3350 cm<sup>-1</sup> (O - H stretching vibrations), 2924cm<sup>-1</sup> (C-H stretching vibrations), 1750 cm<sup>-1</sup> and 1632 cm<sup>-1</sup> (C=O stretching vibrations), and 1416 cm<sup>-1</sup> (C-O-C stretching vibrations), in according to data previously published<sup>19</sup>.

FTIR spectrum of SDSD systems presented an increase of the intensity of the peak at 2250 cm<sup>-1</sup> as the ratio of EFV in these systems increased (Fig. 3). They also showed disappearance of characteristic peak of EFV at 3320 cm<sup>-1</sup> attributed to N-H stretching vibrations (Fig. 3I) and shifting of the peak at 1750 cm<sup>-1</sup> when compared to pure EFV (Fig. 3II). The peaks corresponding to the carbonyl group of vinyl acetate (1730 cm<sup>-1</sup>) and caprolactam (1630 cm<sup>-1</sup>) are broadened. These events may be attributed to a

possible interaction by hydrogen-bonds between the proton accepting groups (C=O) in the Soluplus<sup>®</sup> and the proton donating groups (-NH) of EFV. The disappearing of N-H stretch vibration region of EFV when associated to polymer PVP K30 in solid dispersion has been described in the literature, suggesting to be related to hydrogen bonding interactions<sup>39</sup>.

### **Drug loading, particle size, and shape of SDSD systems**

#### *Drug content*

Drug content for each SDSD powder was consistent with theoretical values (Table 2). Successful drug loading on powders generated by spray drying from solutions (drug and polymer being both dissolved) are commonly reported in the literature<sup>4, 41</sup>.

#### *Particle size and yields*

Particle size is critical in the successful development of solid dispersions since it significantly influences the dissolution. Hence particle size and distribution of the prepared spray-dried solid dispersions collected from the cyclone are given in Table 2. The mean volume diameters  $D[4.3]$  are found to be  $7.7 \pm 0.3$ ,  $6.1 \pm 0.2$  and  $4.2 \pm 0.5$   $\mu\text{m}$  for SDSD1, SDSD2 and SDSD3 respectively, which are significantly different from each other (one way ANOVA,  $p < 0.05$ ). The 90% of particles collected are below  $12.9 \pm 0.4$ ,  $10.8 \pm 0.3$  and  $8.5 \pm 1.3$   $\mu\text{m}$  for SDSD1, SDSD2 and SDSD3, respectively. The small distribution indicated that the size of the dried particles is precisely controlled by atomization pressure and feed rate during the spray drying process. Additionally, the small particle sizes ( $< 12.9$   $\mu\text{m}$ ) could be attributed to the low viscosity of the spraying solution (Table 2) and high compressed nitrogen flow rate.

The percentage yield for spray-dried samples was found to be higher than 70%, which is relatively high from a laboratory-scale spray dryer.

### *SEM images*

Scanning electron microscopy (SEM) was used to investigate the particle microstructures. Fig 4 represents the SEM images of the unprocessed EFV crystals, spray-dried Soluplus<sup>®</sup> and all SDDS differing in drug: polymer ratio.

The unprocessed EFV crystals (Fig 4a) are elongated, stick-like, and quite regular in their multi-face geometry. Spray-dried EFV was not observed by SEM because, due to its low T<sub>g</sub>, the powder was often sticky and hardly recoverable. Spray-drying of pure Soluplus<sup>®</sup> resulted in wrinkled particles (Fig 4b). In comparison the “wrinkled collapsed morphology” of drug-loaded SDDS1 and SDDS2 particles (Figs. 4c and 4d) is not affected by the drug presence, except for SDDS3 (Fig 4e).

Polymer mass in the feed solution is constant in the three formulations, whereas drug mass changes. For SDDS1 and SDDS2 the feed solution for spray drying has almost the same total solid concentration (11-11.4% w/w) as without drug (10% w/w) and most of this solid is polymer. Thus, particle formation mechanism cannot be very different, even if polymer and drug interact

In contrast, with SDDS3 there is 18% (w/w) of total solid in the feed. Such amount is almost half polymer and half drug. SDDS3 particles are mostly spherical with seemingly smooth surfaces without visible pores and other major surface discontinuities.

Peclet number in the spraying solution helped to understand the ‘deviation’ from wrinkled morphology of the spray-dried SDDS3 particles. The Peclet number is a function of the ratio between solvent evaporation rate ( $k$ ) and the diffusion coefficient of the given solute ( $D$ ):  $Pe \propto k/D$ <sup>42</sup>. The feed concentration has a direct impact on the

Peclet number (namely, on the evaporation rate). When the feed concentration was 10-11.4% w/w (pure polymer, SDDS1 and SDDS2 systems), the skin remained wet for a longer time, so that the hollow particles could deflate and shrivel as it cooled. However, for SDDS3 system, the increase in feed concentration to 18% (w/w) of total solid could help droplets to rapidly develop a dry, hard skin, preventing subsequent deflation and shrinkage.

### *Solubility studies*

Table 3 summarizes the experimentally determined solubility of EFV in pure water, water containing 0.25% (w/v) SLS and biorelevant medium (FeSSIF). As per literature, the solubility of unprocessed EFV crystals in water is less than 10  $\mu\text{g/ml}$ <sup>43</sup>. Experimentally, it was found to be  $1.74 \pm 0.06$   $\mu\text{g/ml}$  at 37°C. The drug solubility in water was increased by the addition of 0.25% (w/v) SLS ( $350.11 \pm 8.90$   $\mu\text{g/ml}$ ) and, in FeSSIF medium it was found to be  $879.89 \pm 23.03$   $\mu\text{g/ml}$ , indicating that EFV exhibited higher solubility in biorelevant medium, i.e. 500 times higher than that of pure EFV in water.

The log P of EFV is 5.4, indicating its high lipophilicity. Sodium taurocholate and lecithin are natural surfactants present in FeSSIF medium, forming more complex lipid aggregates than the micelles formed with synthetic surfactants such as SLS<sup>44</sup>. Hence, we can attribute the higher solubility of EFV in FeSSIF medium to a synergistic effect of sodium taurocholate and lecithin that led to a significant improvement in solubility of EFV by micellar solubilization.

From the data obtained, it is clear that the apparent solubility of the drug was markedly increased in the three aqueous media when EFV was formulated as SDDS binary systems. These results can be explained by the amphiphilic chemical structure of

Soluplus<sup>®</sup> having large number of hydroxyl groups, which make it a good solubilizer for poorly soluble drugs in aqueous media<sup>45</sup>.

The enhanced effect on the apparent drug solubility is also given in terms of the solubility enhancement ratio ( $ER_{sol}$ ) in Table 3. EFV solubility in water, pure and with SLS increased with the increase in polymer proportion (co-solvent effect). A 1:7 proportion showed a maximum increase in apparent solubility ( $4330.66 \pm 21.89 \mu\text{g/ml}$ ) in water containing 0.25% (w/v) SLS equivalent to increase of 12 times ( $ER_{sol}$ ), with respect to pure EFV. Surprisingly, the increased polymer concentration did not show any significant increase ( $p > 0.05$ ) in the apparent solubility of EFV in FeSSIF medium, presumably due to the higher variability of experimental values (high standard deviations).

### ***In vitro* drug dissolution**

The dissolution performance of solid dispersions is very complex as many phenomena take place simultaneously: dissolution of amorphous material, nucleation and growth of the stable form, dissolution of the polymer. Consequently it is relevant to investigate whether the combination of EFV and Soluplus<sup>®</sup> in SDS systems can contribute to enhance dissolution. The dissolution profiles of unprocessed EFV crystals and SDS formulations were determined in purified water containing 0.25 (w/v) % SLS and in FeSSIF medium, at  $37^{\circ}\pm 0.5^{\circ}\text{C}$ . The comparison of dissolution profiles in the two different media (Figs. 5a and 5b) revealed that differences in dissolution performance exist. The concentration of Soluplus<sup>®</sup> was also influencing the dissolution performance of EFV. The quantitative interpretation of the values obtained in dissolution assays is easier using mathematical equations to describe the release profiles (dissolution efficiency parameter and curve-fitting).

#### *Dissolution efficiency (DE)*

Dissolution efficiency within 120 min ( $DE_{120}$ ) is shown in Table 4 and was used as comparison of dissolution profiles. All the solid dispersions prepared gave rapid and higher dissolution of EFV when compared to unprocessed drug crystals. For example, at drug load of 10% (w/w), the solid dispersion of EFV in Soluplus<sup>®</sup> (SDSD1) demonstrated greatly improved dissolution enhancement ( $> 87\%$ , Table 4) which was reduced at higher drug loads (SDSD2, SDS3).

The increase on the dissolution efficiency when increasing the Soluplus<sup>®</sup> concentration can be explained on the basis of the wetting and solubilizing effect of the carrier. A faster release of drug upon lowering the drug load was already observed<sup>46</sup>. However, the

effect of drug loading on the release rate of drugs from solid dispersions is ambiguous as in other studies a faster release of drug was seen at higher drug loads<sup>47</sup>.

A crystalline drug, such as unprocessed EFV crystals shown in Fig. 6, dissolves until the solution concentration reaches the thermodynamic solubility of the drug, after which the concentration remains constant. The amorphous form, on the other hand, initially dissolves more rapidly than the crystalline form and reaches a higher concentration, forming metastable highly supersaturated solutions. The dissolution rate of the drug from amorphous solid dispersion formulations such as the SDDS systems is a critically important factor in dictating the generation and duration of the supersaturated state. Fig. 6 shows that during dissolution in 0.25% (w/v) SLS, in comparison to unprocessed EFV crystals, the three SDDS systems were capable of yielding EFV supersaturation in solution with duration of at least 120 min, whereas in FeSSIF medium, the most concentrated SDDS in drug (SDDS3) yielded EFV concentration in solution close to the EFV concentration entering in solution from the dissolution of the crystalline form (unprocessed EFV crystals).

It has been demonstrated that hydrophobic groups on modified polymers, such as the amphiphilic polymer Soluplus<sup>®</sup>, can interact hydrophobically with hydrophobic drugs<sup>48</sup>. FT-IR analysis has indicated possible interactions between EFV and Soluplus<sup>®</sup>, which could partly explain the reduction of the rate with which the drug dissolves, as observed for the SDDS3 system in both media. Moreover, the lower EFV concentrations found in the FeSSIF medium from SDDS3 could be attributed, in part, to another reason: prevention of recrystallization is another potential role the polymer may exert to maintain the EFV in solution. Increasing drug load on SDDS reduces the distance between drug molecules and hence facilitates crystallization. It is what probably happened during the dissolution of SDDS3 in FeSSIF medium and the amount

of some crystallized drug within SDS3 decelerated the dissolution of EFV from this solid dispersion.

### *Curve fitting*

To determine the mechanism of drug release, the first 60% drug release data from SDS1, SDS2 and SDS3 formulations were fitted in Korsmeyer–Peppas model<sup>32</sup>. Nonlinear regressions were applied for cumulative dissolved drug. The coefficient of determination ( $R^2$ ), root-mean-square error (RMSE) and Akaike's information criterion (AIC) values were determined using KinetDS 3.0 rev. 2010 software, Krakow, Poland. From the obtained results it is observed that the drug release mechanism is well described mathematically by the Korsmeyer-Peppas equation (Eq. 3), considering the values of  $R^2$ , AIC and RMSE. All values of exponent (n) determined from Korsmeyer-Peppas model were lower than 0.5 (Table 4), suggesting Fickian diffusion<sup>49</sup> as the mechanism of drug release from all formulations. The penetration of the dissolution medium will be controlled by the diffusion through the polymer layer around the drug molecularly dispersed in the solid dispersions.

### **Stability studies**

#### *Dynamic vapor sorption (DVS)*

A water sorption isotherm provides information about the affinity between the material and water. Fig. 6 displays the dynamic vapor sorption (DVS) isotherm plots for the studied samples, showing the percentage change in mass as a function of changing relative humidity. The reversibility of the water uptake was clearly seen in all cases. The slight but constant hysteresis (separation) between the adsorption and desorption isotherms can be due to bulk absorption and desorption limited by the diffusion.



The water sorption isotherm of pure spray-dried Soluplus<sup>®</sup> shows a hygroscopic character with 30.3% change of mass at 95% RH, whereas amorphous EFV shows a hydrophobic character with 0.1% change of mass. All the three formulations evaluated, SDDS1, SDDS2 and SDDS3, showed expected behavior, i.e., the amount of absorbed water in solid dispersions decreased at increasing drug loads (SDDS3<SDDS2<SDDS1), because amorphous EFV is hydrophobic.

To compare samples with different drug loads, the amount of water absorbed in the solid dispersions was corrected for the drug load. The carrier was considered as a separate matrix with certain hygroscopicity. The results are depicted Fig. 7. It can be seen that EFV reduced the water uptake of Soluplus<sup>®</sup> matrix resulting in a linear decrease in hygroscopicity of polymer in solid dispersions with increasing drug loads.

Assuming that there is no interaction between the components, the moisture of a binary mixture can be calculated by the additivity of the individual components. The theoretically calculated values of moisture gains for Soluplus<sup>®</sup> is also given in Fig. 7, as a function of composition. The negative deviations observed for all three compositions suggest the existence of favorable interactions between drug and polymer. The higher deviation seen at higher EFV content (SDDS3) means a stronger interaction toward this composition. The interactions can influence the number of polar functional groups that are available for the possible interaction with water during sorption, as already observed for other solid dispersions with Soluplus<sup>®</sup> or PVP and Valsartan as drug<sup>50</sup>.

#### *Accelerated stability*

Data presented in this paper have shown the positive effect of increasing drug loads from 10% (w/w) (SDDS1) to 44% (w/w) (SDDS3) decreasing the hygroscopicity of the amorphous solid dispersion. Besides, high drug contents are also suitable for the preparation of high dosed dosage forms, as in the case of EFV. On the other, the

increase of drug loading can generate a negative effect, impairing the physical stability by reducing the distance between drug molecules and hence facilitating crystallization. It is difficult to predict what these effects will be predominant. To investigate this, SDDS3 was exposed to 40°C/75%RH until its moisture content reached equilibrium under these conditions; then it was immediately analyzed by DSC and Raman microscopy mapping. In this experiment, SDDS3 gained 2.9% (w/w). This humidity reduced T<sub>g</sub>, but was not capable to induce phase separation under the storage conditions, as evidenced by the single T<sub>g</sub> (Table 5).

In addition to the DSC, the distribution of amorphous drug and polymer in the solid dispersion could be evaluated using Raman mapping. For this, surface (10\*10µm) and deep spectra (12\*10µm) have been taken to accurately determine the distribution of the drug and of the polymer. The analysis of the spectra presented on Fig. 8 (peaks between 3000 and 3130 cm<sup>-1</sup>), confirmed that amorphous drug and polymer phases are indistinguishable, as the drug and polymer are miscible with each other in one phase.

#### *Long-term stability*

To evaluate the stability of aged SDDS samples, SDDS systems containing the lower (SDDS1) and the higher (SDDS3) drug loads (10% and 44%, respectively) were characterized by DSC after storage for 12 months at room temperature (~22°C) and 23% RH. For both samples, the XRD spectra (Fig. 9) were similar to that obtained with freshly prepared formulations, and no drug crystallization was observed after one year of storage under the set conditions. Modulated DSC analysis also confirmed the existence of a single T<sub>g</sub> (Table 5), indicating that EFV remained amorphous in these two formulations under the storage conditions. These results may be due to the fact that Soluplus<sup>®</sup> can engage in hydrogen bonding with EFV, resulting in less molecular

mobility and retarded crystallization during storage under the studied conditions. The gradual increase in  $T_g$  over time seen in Table 5 was presumably due to drying of the sample over desiccant.

## **Conclusion**

In the current work, it was clearly demonstrated that amorphous solid dispersion of EFV in Soluplus<sup>®</sup> (SDSD systems) can be effectively produced by spray-drying with enhanced solubility and dissolution rate. The dissolution of the SDSD systems led to sustained supersaturation within 120 min in FeSSIF medium, the value of which varied depending on the drug loading used in the formulation.

SDSD loaded with 10% (w/w) of EFV was the most efficient system, improving EFV solubility in FeSSIF medium 2-fold, assuring a dissolution efficiency of  $86.75 \pm 0.16\%$  with sustained supersaturation within 120 min (compared to  $28.20 \pm 2.67\%$  of unprocessed EFV crystals), and was shown to be physically stable for one year at 22°C when protected from moisture.

## **Acknowledgments**

The authors acknowledge Gala<sup>®</sup> technological platform (France) for technical support, Brazilian Research Council for Scientific and Technological Development (CNPq) for providing PhD Research Fellowship to the first author. The authors are grateful to S. Delconfetto, . Patry, C. Rolland and L. Haurie from Rapsodee Centre for respectively DSC, DVS, SEM and Raman experimental help and analyses.

## **Declaration of interest**

The authors report no conflicts of interest regarding this manuscript.

## References

1. Chiappetta DA, Alvarez-Lorenzo C, Rey-Rico A, Taboada P, Concheiro A, Sosnik A. N-alkylation of poloxamines modulates micellar assembly and encapsulation and release of the antiretroviral Efavirenz. *Eur J Pharm Biopharm.* 2010a;76(1): 24–37. doi: 10.1016/j.ejpb.2010.05.007
2. Pereira SA, Branco T, Caixas U, Côrte-Real RM., Germano I, Lampreia F, Monteiro EC. Intra-individual variability in efavirenz plasma concentrations supports therapeutic drug monitoring based on quarterly sampling in the first year of therapy. *Ther Drug Monit.* 2008;30(1): 60-66. doi: 10.1097/FTD.0b013e318160ce76.
3. Madhusudhan A, Reddy B, Venkatesham M, Veerabhadram G. Design and evaluation of efavirenz loaded solid lipid nanoparticles to improve the oral bioavailability. *Int J Pharm Pharm Sci.* 2012;2(4):84-89.
4. Katata L, Tshweu L, Naidoo S, Kalombo L, Swai H. Design and formulation of nano-sized spray dried efavirenz-part I: Influence of formulation parameters. *J Nanoparticle Res.* 2012;14(11).
5. Seremeta KP, Chiappetta DA, Sosnik A. Poly( $\epsilon$ -caprolactone), Eudragit<sup>®</sup>RS 100 and poly( $\epsilon$ -caprolactone)/Eudragit<sup>®</sup>RS 100 blend submicron particles for the sustained release of the antiretroviral efavirenz. *Colloids Surf., B Biointerfaces.* Elsevier B.V.; 2013;102:441–9. doi: 10.1016/j.colsurfb.2012.06.038
6. Pinto EC. Estudo de dissolução intrínseca de Efavirenz como ferramenta para antecipação de sua biodisponibilidade. Faculdade de Farmácia, Universidade

Federal do Rio de Janeiro, Rio de Janeiro, 2012.

7. da Costa MA, Seiceira RC, Rodrigues CR, Hoffmeister CRD, Cabral LM, Rocha HVA. Efavirenz Dissolution Enhancement I: Co-Micronization. *Pharmaceutics*. 2013;5(1):1–22. doi: 10.3390/pharmaceutics5010001.
8. Patel GV, Patel VB, Pathak A, Rajput SJ, Nanosuspension of efavirenz for improved oral bioavailability: formulation optimization, in vitro, in situ and in vivo evaluation. *Drug Dev Ind Pharm*. 2014;40(1):80–91. doi: 10.3109/03639045.2012.746362.
9. Chadha R, Arora P, Bhandari S, Jain DVS. Effect of hydrophilic polymer on complexing efficiency of cyclodextrins towards efavirenz-characterization and thermodynamic parameters. *J Incl Phenom Macrocycl Chem*. 2012a ;72(3-4):275–87, 2012a. doi: 10.1007/10847-011-9972-z.
10. Lamba SS, Chowdary KPR. A factorial study on formulation development of efavirenz tablets employing  $\beta$  Cyclodextrin- Poloxamer 407- PVPK30. *IJPSR*. 2012;3(3): 782-787.
11. Chiappetta DA., Hocht C., Taira C., Sosnik A. Efavirenz-loaded polymeric micelles for pediatri anti-HIV pharmacotherapy with significantly higher oral bioavailability *Nanomed*. 2010b;5(1):11–23. doi: 10.2217/nmm.09.90.
12. Deshmukh A, Kulakrni S. Novel Self Micro-emulsifying drug delivery systems (SMEDDS) of Efavirenz. *J Chem Pharm Res*. 2012;4(8):3914–19.
13. Chadha R, Saini A, Arora P, Chanda S, Dharamvirsinghain. Cocrystals of efavirenz with selected conformers: Preparation and characterization. *Int J Pharm Pharm Sci*. 2012b;4(2):244–50.

14. Madhavi BB, Chatanya, CK, Madhu, MN, Harsha, VS, Banji, D. Dissolution enhancement of efavirenz by solid dispersion and PEGylation techniques. *Int J Pharm Investig.* 2011;1(1):29-34.
15. Venkateswara-Reddy B, Ramana-Murthy KV. Enhancement of dissolution rate of efavirenz by solid dispersion technique. *IJPBS.* 2012;2(2):185-90.
16. Alves LDS., de La Roca Soares MF., de Albuquerque CT., et al. Solid dispersion of efavirenz in PVP K-30 by conventional solvent and kneading methods. *Carbohydr Polym.* 2014;104: 166–74. doi: 10.1016/j.carbpol.2014.01.027.
17. Sathigari SK, Radhakrishnan VK, Davis VA, Parsons, DL, Babu RJ. Amorphous-State Characterization of Efavirenz-Polymer Hot-Melt Extrusion Systems for Dissolution Enhancement. *J. Pharm. Sci.* 2012;101(9): 3456–64.
18. Chowdary KPR., Enturi V. Preclinical pharmacokinetic evaluation of Efavirenz solid dispersions in two new modified starches. *J Appl Pharm Sci.* 2013;3(4): S89–92. doi: 10.7324/JAPS.2013.34.S17.
19. Shamma RN, Basha M. Soluplus<sup>®</sup>: A novel polymeric solubilizer for optimization of Carvedilol solid dispersions: Formulation design and effect of method of preparation. *Powder Technol;* 2013;237: 406–14. doi: 10.1016/j.powtec.2012.12.038.
20. Reintjes T, Koltzenburg S, Karl M, Schönherr M, Herting MG, Nguyen-Kim V. Solubility enhancement with BASF Pharma polymers - Solubilizer compendium. 2011. 128 p.
21. Dhirendra K, Lewis S, Udupa N, Atin K. Review Solid Dispersions: a Review. *Pak J Pharm Sci.* 2009; 22(2): 234–246.

22. Dobry DE, Settel DM, Baumann JM, Ray, RJ, Graham LJ, Beyerinck RA. A Model-Based Methodology for Spray-Drying Process Development. *J Pharm Innov.* 2009;4(3): 133–42. doi: 10.1007/s12247-009-9064-4
23. Repka MA, Shah S, Lu J, Maddineni S, Morott J, Patwardhan K, Mohammed NN. Melt extrusion: process to product. *Expert Opin Drug Deliv.* 2012;9(1): 105–25. doi: 10.1517/17425247.2012.642365
24. Paudel A, Worku ZA, Meeus J, Guns S, Van Den Mooter G. Manufacturing of solid dispersions of poorly water soluble drugs by spray drying: Formulation and process considerations. *Int J Pharm.* 2013;453: 253–84. doi: 10.1016/j.ijpharm.2012.07.015
25. Hansen CM. Hansen Solubility Parameters. A user's handbook. Boca Raton: CRC Press (2007). 2ed.
26. Van Krevelen DW, Hoftyzer PJ. Properties of polymers. Their estimation and correlation with chemical structures. New York: Elsevier. (1976). 2ed
27. Gordon M, Taylor JSJ. *Appl. Chem.* 1952; 2:493–500
28. USP35. United States Pharmacopeia 35 - National Formulary 30. 2012.
29. Panikumar A Sunitha G, Venkat Raju Y, Sathesh Babu PR., Subrahmanyam CVS. Development of Biorelevant Efavirenz and Its Formulations. *Asian J Pharm Clin Res.* 2012;5(3): 220-223.
30. Kuentz M. Drug absorption modeling as a tool to define the strategy in clinical formulation development, Towards Integrated ADME Prediction: Past, Present, and Future. *AAPS J.* 2008;10(3): 473–79. doi: 10.1208/s12248-008-9054-3
31. Mendyk A, Jachowicz R, Fijorek K, Dorozynski P, Kulinowski P, Polak S.

- KinetDS: An Open Source Software for Dissolution Test Data Analysis. *Dissolution Technol.* 2012;19(1): 6–11.
32. Korsmeyer RW, Gurny R, Doelker E, Buri P, Peppas NA. Mechanisms of solute release from porous hydrophilic polymers. *Int J Pharm.* 1983;15(1): 25–35. doi: 10.1016/0378-5173(83)90064-9.
  33. Greenhalgh DJ, Williams AC, Timmins P, York P. Solubility parameters as predictors of miscibility in solid dispersions. *J Pharm Sci.* 1999;88(11): 1182–90.
  34. Mahapatra S, Thakur TS, Joseph S, Varughese S, Desiraju GR. New solid state forms of the anti-HIV drug efavirenz. Conformational flexibility and high Z' issues. *Cryst Growth Des.* 2010;10(7): 3191–202. doi: 10.1021/cg100342k
  35. Yu M, Ocando JE, Trombetta L, Chatterjee, P. Molecular Interaction Studies of Amorphous Solid Dispersions of the Antimelanoma Agent Betulinic Acid. *AAPS PharmSciTech.* 2014;16(2): 384–397. doi: 10.1208/s12249-014-0220-x
  36. Zallen R. The formation of amorphous solids. In: *The Physics of amorphous solids.* New York: Wiley; 1983. 1–22
  37. Janssens S, De Zeure A, Paudel A, Van Humbeeck J, Rombaut P, Van den Mooter G. Influence of Preparation Methods on Solid State Supersaturation of Amorphous Solid Dispersions: A Case Study with Itraconazole and Eudragit E100. *Pharm Res.* 2010;27(5): 775-85. doi: 10.1007/s11095-010-0069-y.
  38. Homayouni A, Sadeghi F, Nokhodchi A. Preparation and characterization of celecoxib dispersions in Soluplus<sup>®</sup>: Comparison of spray drying and conventional methods. *Iran J Pharm Res.* 2015;14(1): 35–50.



39. Koh PT, Chuah JN, Talekar M, Gorajana A, Garg S. Formulation development and dissolution rate enhancement of efavirenz by solid dispersion systems. *Indian J. Pharm. Sci.*. 2013; 75(3): 291–301.
40. Wang FJ, Wang CH. Sustained release of etanidazole from spray dried microspheres prepared by non-halogenated solvents. *J Control Release*. 2002;81(3): 263–80. doi: 10.1016/S0168-3659(02)00066-4.
41. Rassa G, Gavini E, Spada G, Giunchedi P, Marceddu E. Ketoprofen spray-dried microspheres based on Eudragit® RS and RL: Study of the manufacturing parameters. *Drug Dev. Ind. Pharm.* 2008;34(11): 1178-87. doi: 10.1080/03639040801974303
42. Vehring R. Pharmaceutical particle engineering via spray drying. *Pharm Res*. 2008;25(5): 999-1022. doi: 10.1007/s11095-007-945-1.
43. Maurin MB, Rowe SM, Blom K, Pierie ME. Kinetics and mechanism of hydrolysis of efavirenz. *Pharm. Res*. 2002;19: 517–522. doi: 10.1023/A:1015160132290
44. Iardia-Arana D, Kristensen HG, Müllertz A. Biorelevant dissolution media: aggregation of amphiphiles and solubility of estradiol. *J. Pharm. Sci.* 2006 ;95(2): 248–55. doi: 10.1002/jps.20494.
45. Thakral NK, Ray AR, Bar-Shalom D, Eriksson AH, Majumdar DK. Soluplus-Solubilized Citrated Camptothecin—A Potential Drug Delivery Strategy in Colon Cancer. *AAPS PharmSciTech*. 2012;13(1):59–66. doi:10.1208/s12249-011-9720-0.
46. Torrado S, Torrado S, Torrado JJ, Cadorniga R. Preparation, dissolution and characterization of albendazole solid dispersions. *Int J Pharm*. 1996;140:247–250. doi: 10.1016/0378-5173(96)04586-3.

47. Zingone G, Rubessa, F. Release of carbamazepine from solid dispersions with polyvinylpyrrolidone/vinylacetate copolymer (PVP/VA). *STP. Pharma Sci*, 1994;4(2): 122-127.
48. Wahlgren M, Christensen KL, Jorgensen EV, Svensson A, Ulvenlund S. Oral-based controlled release formulations using poly (acrylic acid) microgels. *Drug Development and Industrial Pharmacy*, 2009;35(8): 922-929.
49. Singhvi, G.; Singh, M. Review: in vitro drug release characterization models. *Int J Pharm Stud Res*. 2011;2(1): 77–84.
50. Punčochová K, Heng JYY, Beránek J, Štěpánek F. Investigation of drug–polymer interaction in solid dispersions by vapour sorption methods *Int J Pharm*. 2014;469(1): 159–67. doi: 10.1016/j.ijpharm.2014 04 048.

## List of figures

Figure 1. DSC thermograms of Soluplus®; unprocessed EFV crystals; physical mixture (EFV:Soluplus® 1:1.25) and spray-dried EFV:Soluplus® solid dispersions: SDS3 (1:1.25); SDS2 (1:7); SDS1 (1:10).

Figure 2. X-ray diffractograms of unprocessed EFV crystals, Soluplus® and spray-dried EFV:Soluplus® solid dispersions (SDS1 1:10, SDS2 1:7 and SDS3 1:1.25).

Figure 3. Fourier transform infrared spectra of (a) Soluplus®; (b) unprocessed EFV crystals; (c) SDS1 1:10; (d) SDS2 1:7; (e) SDS3 1:1.25. Zoom into some regions of the FTIR spectra: I. 4000-2600  $\text{cm}^{-1}$ , revealing disappearance of EFV peak at 3320  $\text{cm}^{-1}$ ; II. 1900-1550  $\text{cm}^{-1}$ , revealing shifting of EFV peak at 1750  $\text{cm}^{-1}$ .

Figure 4. SEM images of (a) unprocessed EFV crystals, (b) spray-dried Soluplus®, (c) SDS1 1:10, (d) SDS2 1:7, (e) SDS3 1:1.25.

Figure 5. Dissolution profiles of unprocessed EFV crystals and SDS powders in two different dissolution media: aqueous media containing (a) SLS 0.25 (w/v) %; (b) and simulated intestinal fluid en fed state (FeSSIF pH 5.0) medium.

Figure 6. Dynamic vapor sorption (DVS) isotherms for spray-dried Soluplus®, spray-dried EFV and SDS formulations.

Figure 7. Water vapor sorption in Soluplus® in SDS systems as a function of EFV content. The solid line represents the theoretical moisture gains calculated as a function of composition.

Figure 8. Image of the scanned area and Raman microscopic mapping correspondent for SDS3 sample with peaks of EFV and Soluplus® (peaks between 3000 and 3130  $\text{cm}^{-1}$ ).

Figure 9. X-ray diffractograms of unprocessed EFV crystals, SDS1 (1:10) and SDS3 (1:1.25), after 1 year storage at room temperature ( $\sim 22^\circ\text{C}$ ), protected from moisture (23%RH).

Figure 1

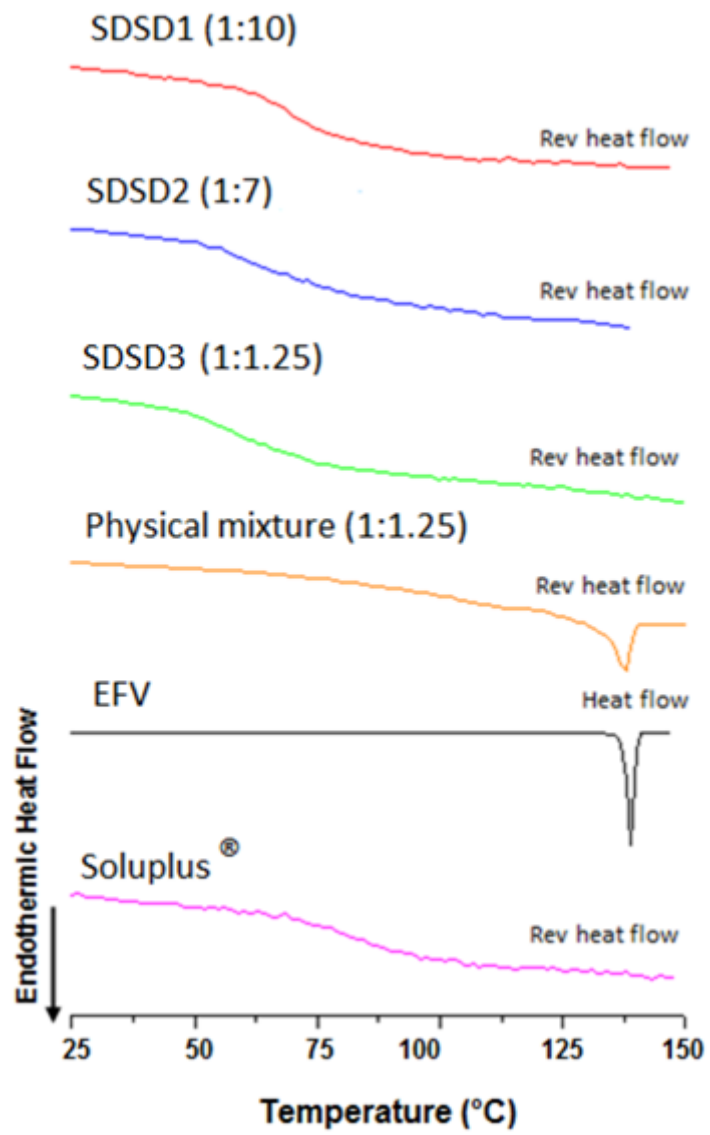


Figure 2

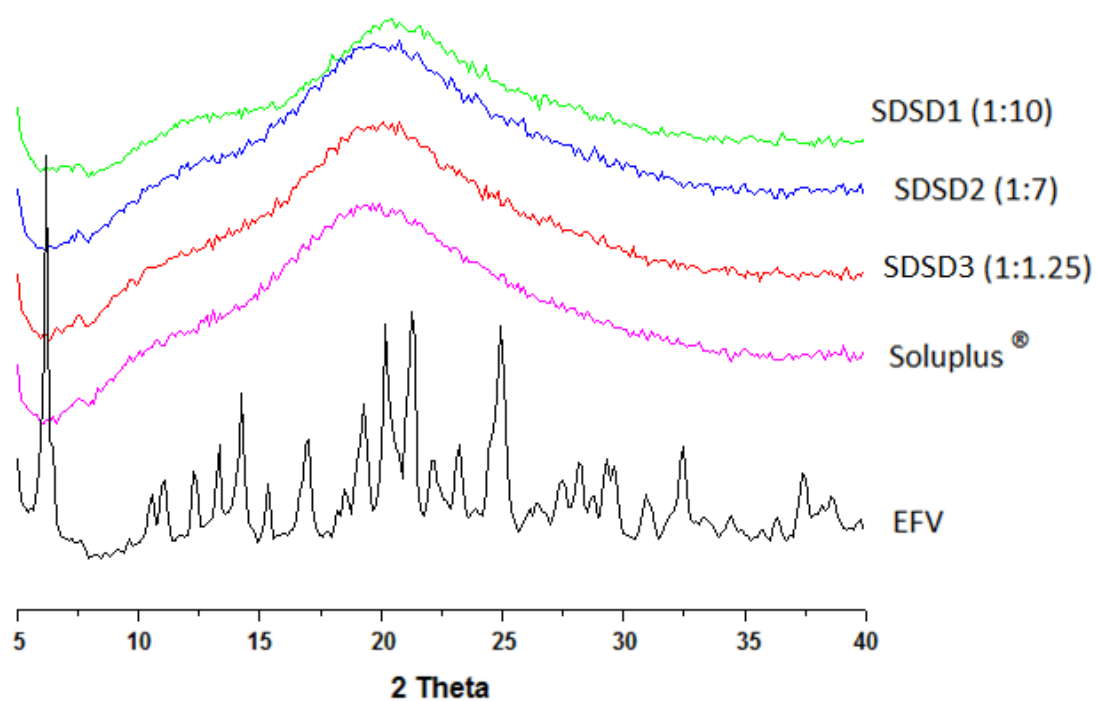


Figure 3

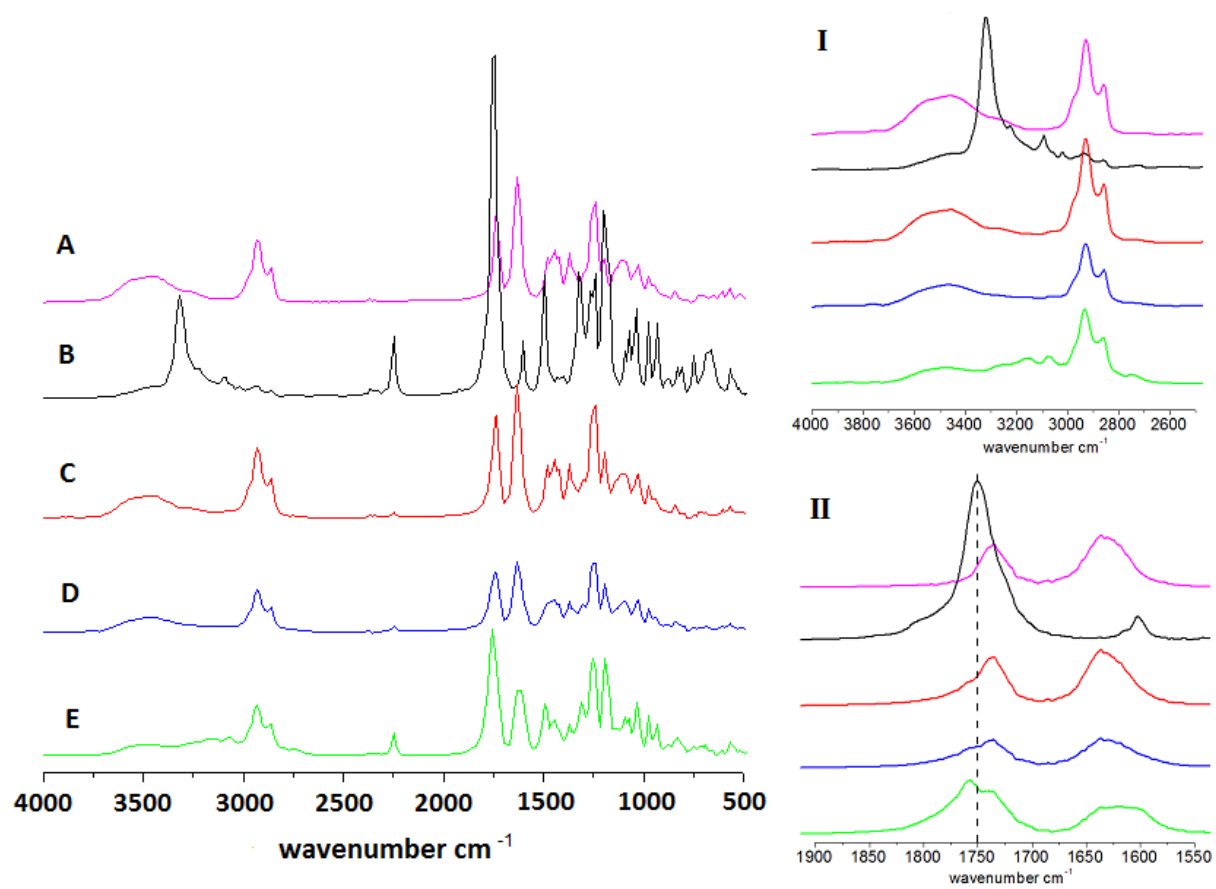


Figure 4

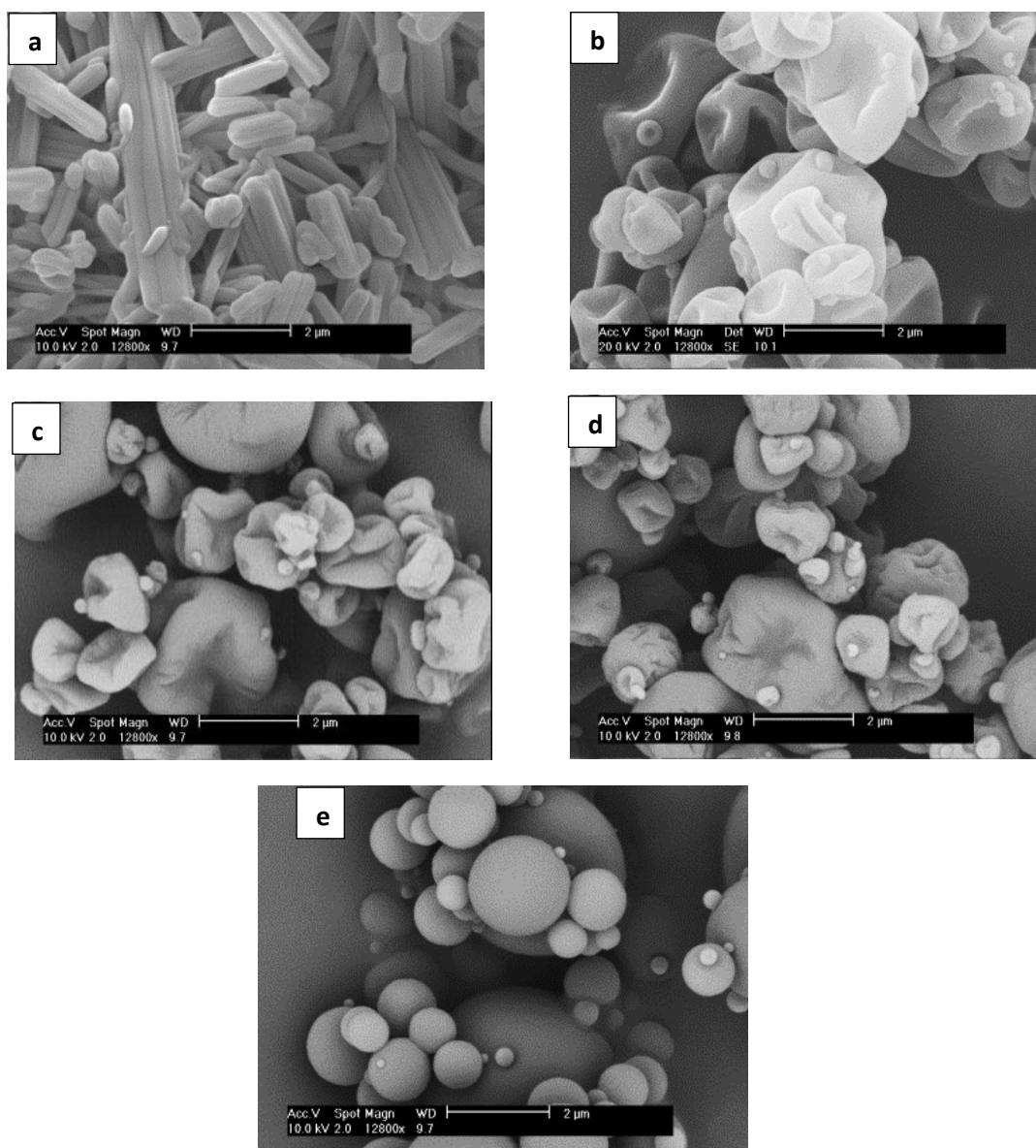


Figure 5

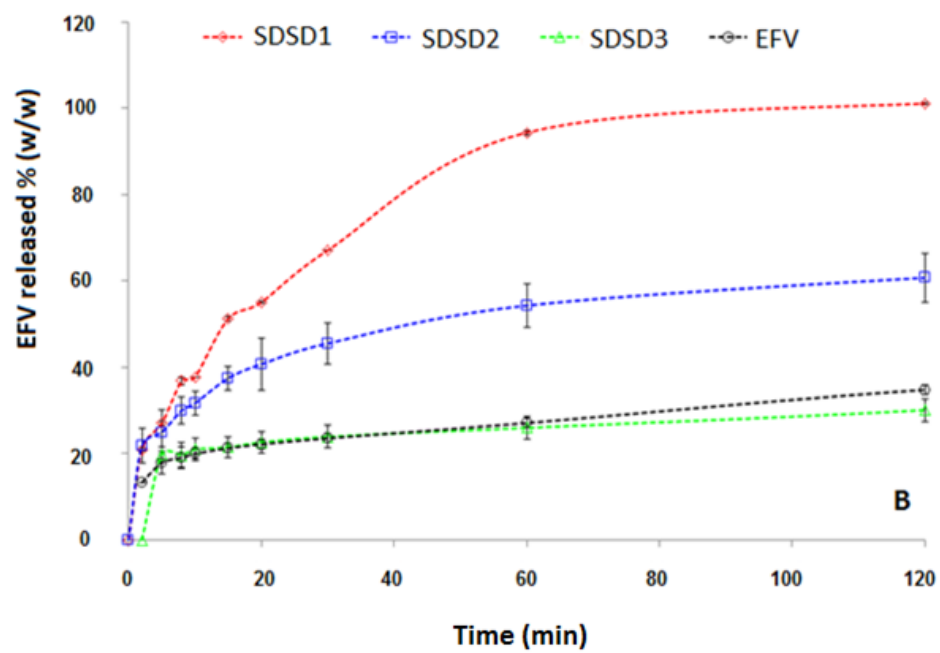
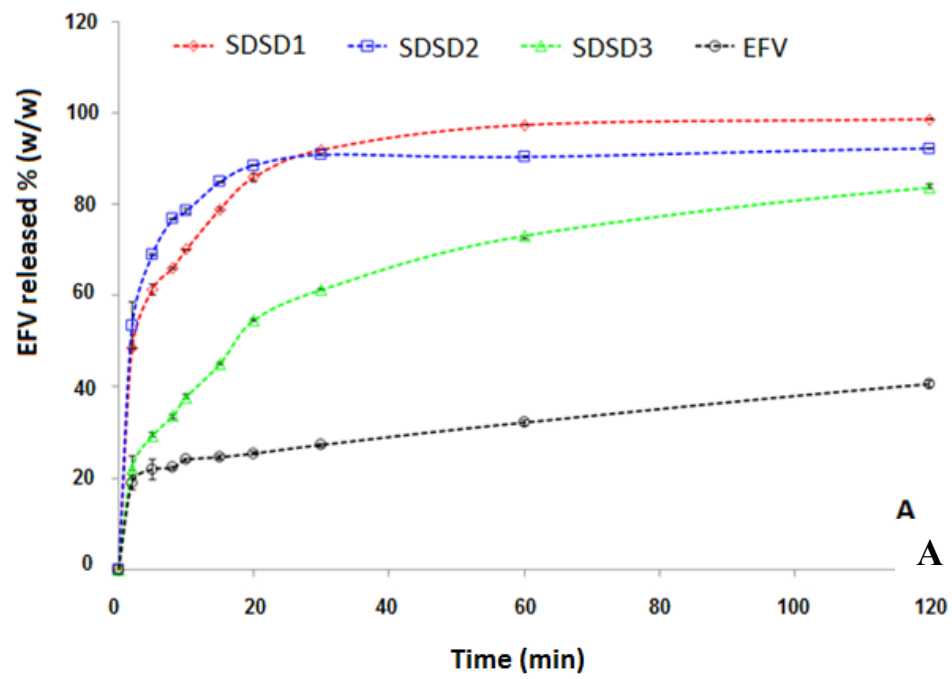


Figure 6

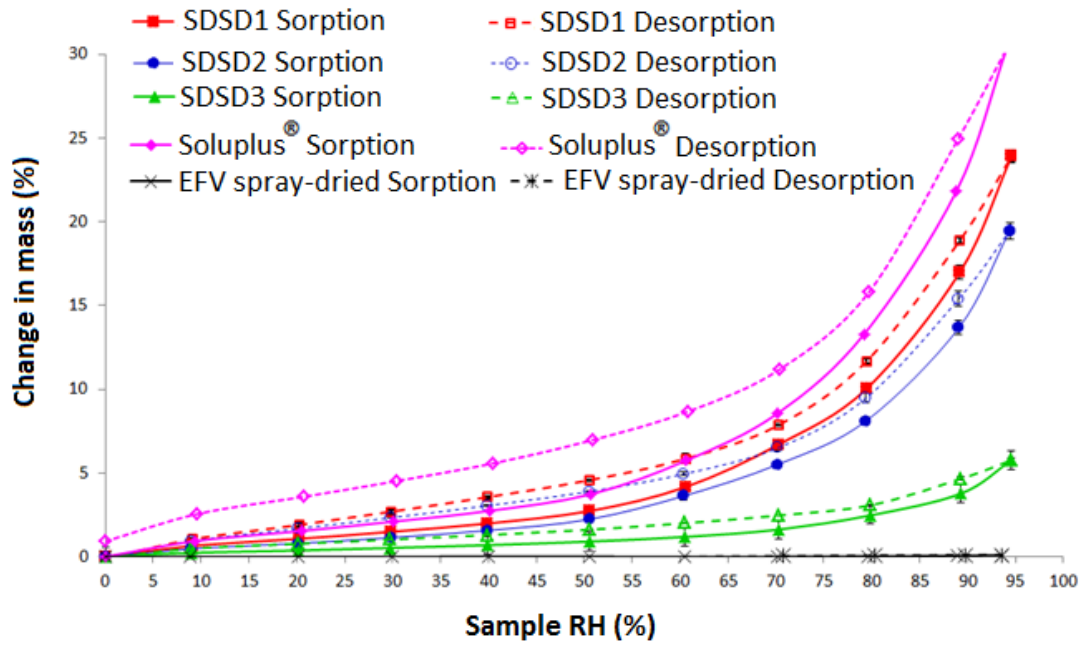


Figure 7

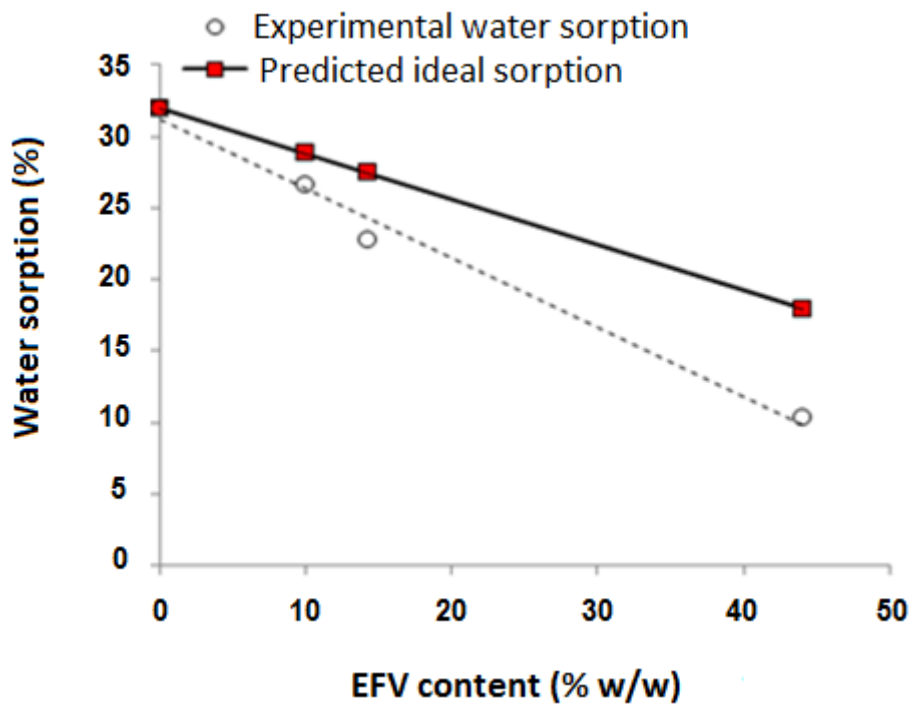




Figure 8

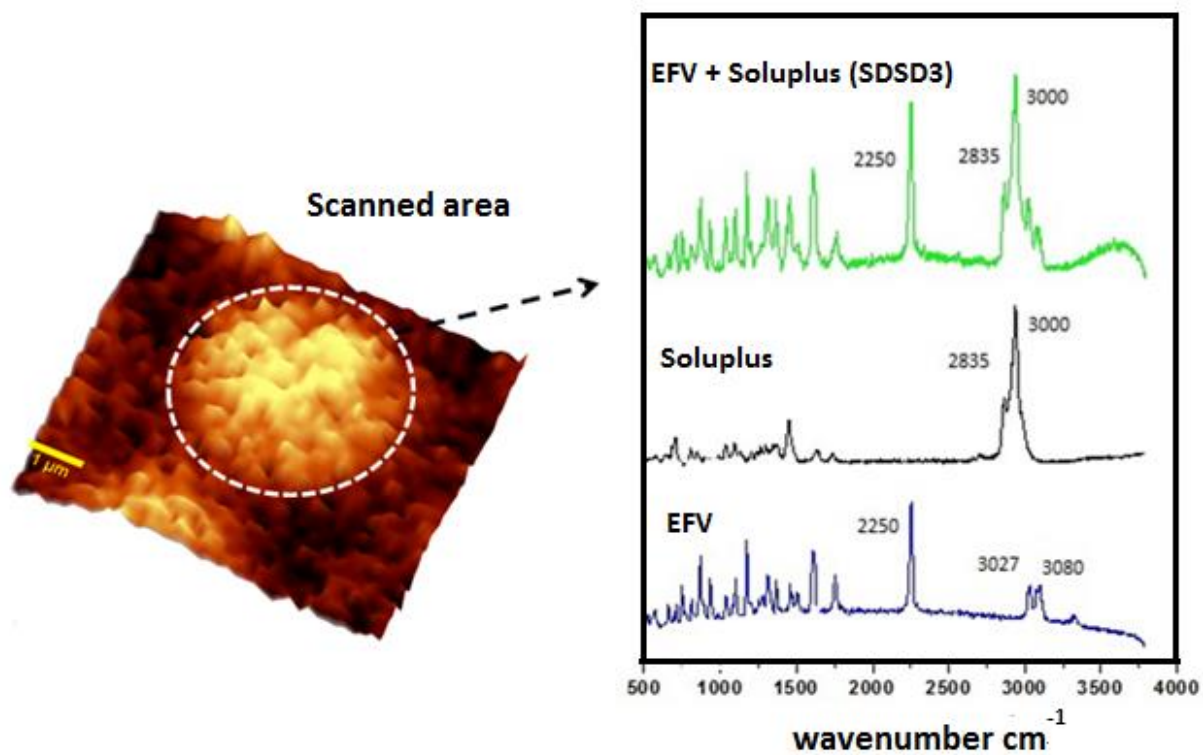
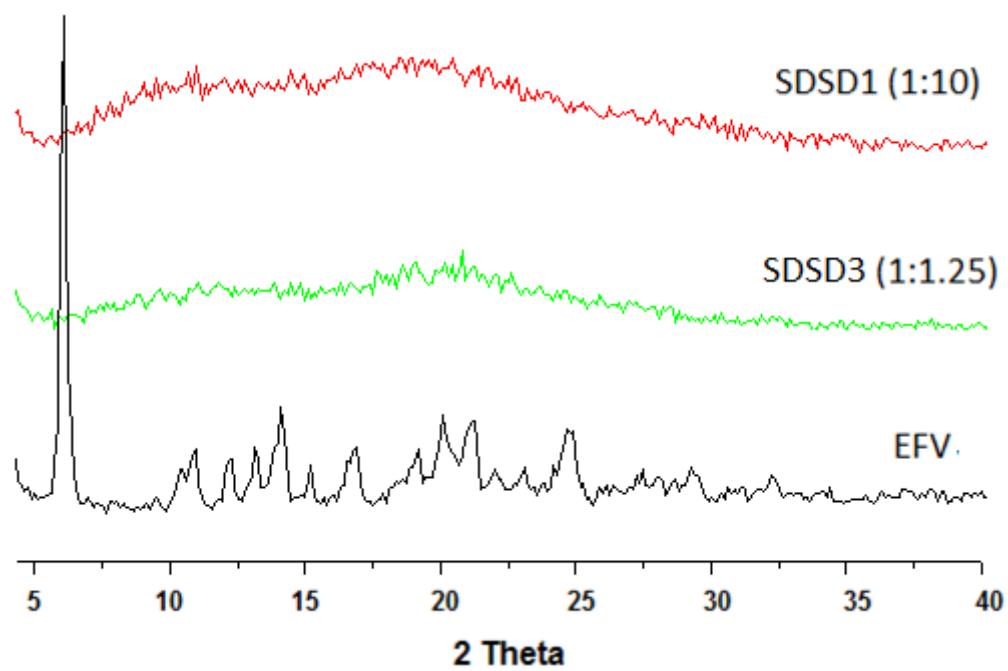


Figure 9



## **List of tables**

Table 1. Thermal properties of EFV, Soluplus<sup>®</sup> and SDDS systems: experimental data from DSC/mDSC and theoretical values (Gordon-Taylor equation).

Table 2. Characteristics of feed solutions and SDDS systems.

Table 3. Solubility of unprocessed EFV crystals and SDDS systems at 37°C in three different aqueous media

Table 4. Dissolution efficiency (DE<sub>120</sub>) and kinetic analysis of *in vitro* dissolution using the Korsmeyer- Peppas model.

Table 5. T<sub>g</sub> of the SDDS systems under various storage conditions.

Table 1

Sample	$T_m$ (°C)	$T_g$ (°C)	$\Delta C_p$ (J/g.K)	$T_g$ Gordon-Taylor (°C)	$\Delta T_g$
EFV*	139.2	35.5**	0.26	-	-
Spray-dried EFV	-	36.1	0.32	-	-
Spray-dried Soluplus®	-	78.8	0.12	-	-
SDSD1	-	62.3	-	72.7	-10.4
SDSD2	-	56.9	-	70.2	-13.3
SDSD3	-	58.1	-	59.5	-1.4

\* Unprocessed EFV crystals

\*\*  $T_g$  value obtained from heat-cool-heat DSC cycle at 5°C/min in a non-hermetic pan.

Table 2.

Sample	Feed solution	Yield (%)	Spray-dried powder characteristics				
	Viscosity (mPa.S)		Theoretical EFV content (%)	EFV content*	Particle size * ( $\mu$ m)		
					Dv10	D[4,3]	Dv90
SDSD1	9.9 (0.0035)	71.1 (1.04)	10	10.0 (0.1)	3.5 (0.6)	7.7 (0.3)	12.9 (0.4)
SDSD2	9.9 (0.0028)	77.3 (1.09)	15	14.3 (0.1)	2.5 (0.4)	6.1 (0.2)	10.8 (0.3)
SDSD3	9.8 (0.0025)	71.3 (1.01)	45	44.1 (0.7)	1.0 (0.0)	4.2 (0.5)	8.5 (1.3)

\*Mean (and standard deviation in parentheses)

Table 3

Dissolution medium	Solubility* ( $\mu\text{g/ml}$ ) at $37^{\circ}\pm 0.5^{\circ}\text{C}$			
	EFV***	SDSD1	SDSD2	SDSD3
<i>EFV : Soluplus® (w : w)</i>	<b>1 : 0</b>	<b>1 : 10</b>	<b>1 : 7</b>	<b>1 : 1.25</b>
Purified water	1.74 (0.06) (n=2)	15.95 (0.93) (n=2)	14.28 (0.08) (n=2)	9.97 (1.38) (n=2)
ER <sub>sol</sub> **	-	9	8	6
Water containing SLS (0.25% w/v)	350.11 (8.90) (n=3)	3088.32 (47.63) (n=3)	4330.66 (21.89) (n=3)	1022.44 (3.22) (n=3)
ER <sub>sol</sub> **	-	9	12	3
FeSSIF	879.89 (23.03) (n=3)	1698.1 (422.80) (n=2)	1365.55 (246.75) (n=2)	1241.04 (146.75) (n=2)
ER <sub>sol</sub> **	-	2	1.5	1.4

\* Mean (and standard deviation in parentheses)

\*\* ER<sub>sol</sub>: Solubility enhancement ratio

\*\*\* Unprocessed EFV crystals

Table 4.

<b>Dissolution efficiency - DE<sub>120</sub> * (%)</b>							
Water containing SLS (0.25% w/v)				FeSSIF medium			
<b>EFV**</b>	<b>SDSD1</b>	<b>SDSD2</b>	<b>SDSD3</b>	<b>EFV**</b>	<b>SDSD1</b>	<b>SDSD2</b>	<b>SDSD3</b>
35.53 (0.01)	93.77 (0.07)	89.33 (0.11)	73.09 (0.01)	28.20 (2.67) <sup>a</sup>	86.75 (0.16)	50.40 (2.85)	29.33 (2.83) <sup>a</sup>
<b>Korsmeyer- Peppas model</b>							
Curve fitting parameter	Water containing SLS (0.25% w/v)			FeSSIF medium			
	<b>SDSD1</b>	<b>SDSD2</b>	<b>SDSD3</b>	<b>SDSD1</b>	<b>SDSD2</b>	<b>SDSD3</b>	
R <sup>2</sup>	0.9972	0.9981	0.9944	0.9953	0.9842	0.9803	
RMSE	0.86	1.04	2.11	3.58	1.74	1.40	
AIC	12.92	12.43	37.18	58.45	42.62	37.86	
K(min <sup>-1</sup> )	41.24	45.99	16.77	13.66	18.62	14.23	
n	0.23	0.24	0.37	0.47	0.25	0.19	

\* Values represent the mean of two independent determinations.

\*\* Unprocessed EFV crystals

<sup>a</sup> There is no statistical difference (p>0.05).

Table 5

Sample	Drug: Polymer ratio (w:w)	Storage conditions	1 <sup>st</sup> Heating DSC cycle	
			T <sub>g</sub> °C (T <sub>onset</sub> )	ΔC <sub>p</sub> J/g °C
SDSD3	1 :1.25	<i>t</i> <sub>0</sub> (initial)	58.1	0.28
SDSD3	1 :1.25	after water vapor sorption by DVS at 40°C/75% RH	54.7	0.18
SDSD3	1 :1.25	~22°C, 23% RH, 12 months	63.4	0.25
SDSD1	1 :10	<i>t</i> <sub>0</sub> (initial)	62.3	0.22
SDSD1	1 :10	~22°C, 23% RH, 12 months	69.9	0.26